MECHANISMS DESIGN FOR THE HINGE & BATTERY LIFETIME TESTS FOR A PROTOTYPE

Taher Deemyad[1], Vincent Akula[1], Anish Sebastian[1]

[1]Department of Mechanical Engineering, Idaho State University, Pocatello, ID, USA

ABSTRACT

In this paper, we design application specific mechanisms and control systems to test and deduce the lifetime of custom-designed hinges and batteries. These hinges and batteries are critical components of prototypes for a patented smart toilet seat. The work done here was used to improve the existing design and to identify a replacement cycle for these seat components. The target audience for this smart seat is airports and venues with large crowds. The smart seat has a cleaning solution that is contained within the seat in a cartridge, which can be easily replaced by facilities. The seat includes a motion sensor, battery, and slow hinges inside of it. This seat employs a slow hinge which reduces the impact of repetitive opening and closing of the seat. The hinge lifetime was tested and to this end a specific mechanism was designed. In this test, time required for opening seat, closing seat, and total number of opening/closing cycles the seat underwent was recorded. Also, in another experiment, the lifetime of the battery powering the pumping mechanism was tested until failure, where the battery voltage fell below a specific value and could no longer pump the cleaning solution out of the ports. Finally, the results for each experiment were compared for different samples and analyzed.

Keywords: Hinge Lifetime Test, Battery Lifetime Test, Smart Toilet Seat, Mechanism Design, Test Pumping Mechanism, Accelerated Life Testing

1. INTRODUCTION

The smart toilet seat which has been designed as a solution to dirty toilet seats in public restrooms especially high traffic restrooms is estimated to be able to handle high volumes of users within short periods of time. The unit features a soft spring hinge mechanism which guides the closing of the toilet seat as well as a sensor-activated cleaning fluid dispenser mechanism. Both features are critical in the operation of the unit and for the hygiene aspect which this seat is designed to address. A failure of one or both features would result in the failure of the unit to work as advertised.

The hinges and specifically soft hinges are very popular in robotic systems and other smart mechanisms and have multiple advantages compared to revolute joints such as no friction losses and reduced assembly and manufacturing costs [10, 11].

The reliability performance of the toilet seat prototype can be approximated by considering experimental data or historical data analysis of previous models. Historical data analysis is only applicable when the reliability analysis data for previous models is already established [1] after which by means of Weibull analysis, a methodology used for performing life data analysis, the reliability performance can be estimated. However, in this study, data for reliability analysis will be obtained from experimental tests which will be designed to simulate normal use of the product.

Designing the lifetime testing systems includes two major parts: mechanical section and sensors/electrical circuit section. In every electromechanical system, one of the important steps is designing the mechanism with minimum size and number of actuators [16]. This would be more important when there is limitation in workspace [8, 9]. Also, using an optimization method can help designer to find the best size and the most appropriate material for the target structure [7]. There are many sensors that can be used in lifetime testing mechanisms based on the target objective. One of the common sensors are for detecting objects at a specified distance. These sensors vary from LiDAR sensors which are more popular in autonomous vehicles [5] to break-beam sensors in robotic projects [6].

Lithium-ion technologies help us to having batteries with longer lifetime. However, study the lifetime of the batteries and find a proper one is still a challenge [12]. Accurately predicting the lifetime of the batteries is important for ensuring the safety, reliability, and accelerating the battery development cycle. One of the possible methods to reach an accurate early-cycle prediction of battery lifetime, is using machine learning (ML) [13].

FIGURE 1: A WASHIE® TOILET UNIT

It is important to note that the presented smart toilet unit in this research is an innovative design with sensors and automated systems. As the design of a product becomes more involved, so testing reliability becomes more difficult to demonstrate in a reasonable time with a realistic sample size and within a reasonable budget [2]. This problem can be solved by collecting data from the actual use of the toilet seat under normal use. However, the time taken to install the toilet seat at the point of normal use i.e., a public restroom, and observe the failure modes may be impractical. Also, seeing that normal use of the unit is in a location where access is not readily available to the engineer carrying out the experiment, there is need for a more intuitive solution.

The Accelerated Life Testing (ALT) as a test method based on sound engineering and statistical assumptions has been presented in [2]. Also, various statistical models and methods for analyzing ALT data from step-stress tests were discussed in [15] when statistical methods based on imprecise probabilities for ALT was explained in [14]. The objective of ALT is to produce a significant number of failures modes, which must be representative of those that would occur under normal use, within a short period of time [3]. We tried to achieve this in this study by observing the features which, as stated in the preceding paragraphs, would result in the critical failure of the unit. ALT can be applied in the form of overstress acceleration or usage rate acceleration form. The latter is applied in this study. This method is typically applied to devices that do not operate continuously under normal conditions [4]. The type of stress loading applied in the study is the step stress.

2. HINGE SPECIFICATIONS & DESIGN A MECHANISM TO TEST IT

2.1 Hinge test overview

The smart toilet seat in this research is shown in Fig. 1. In this toilet seat, the hinges have a custom filling, which slows down the speed with which the seat closes when installed on a regular toilet bowl (it works primarily using resistance to angular motion). The operation of the hinges involves "opening" and "closing" of the seat multiple times over its lifecycle. Unlike a regular seat hinge, which does not slow down a seat before impacting the bowl, soft hinges provide 2 advantages; a) avoid potential damage of the seat or bowl, due to slamming it shut and b) for aesthetic appeal. For the accelerated life test of the hinges on the Toilet seat, 3 variables were the subject of investigation. Three recorded variables in this work are:

1) *Cycle Number (n = 123…)*
2) *T1 – time from start to finish of "opening" for nth cycle*
3) *T2 – time from start to finish of "closing" for nth cycle*

These variables, after close study of the procedural operation have been selected for this research (Fig. 2).

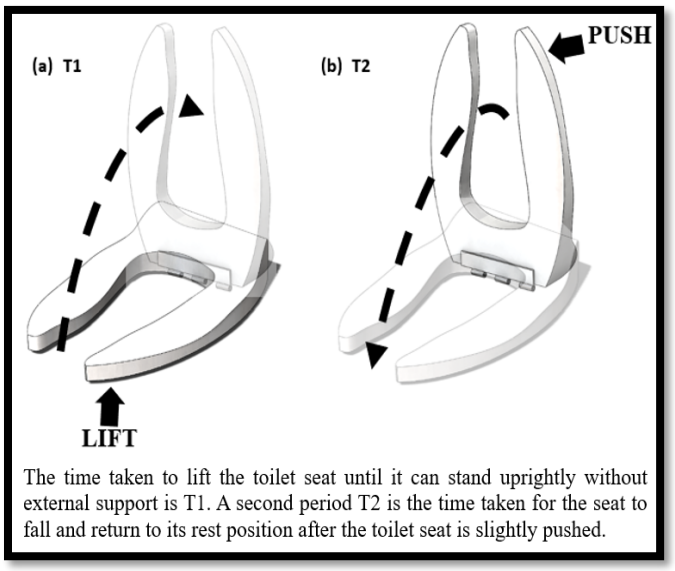

FIGURE 2: THE TWO PERIODS OF EACH CYCLE

In general, a full operation of a toilet seat can be segmented into 2 stages: opening and closing. Therefore, these two actions, while keeping record of the time durations, have to be considered in designing a proper mechanism to test the operation process.

For testing the lifetime of these hinges and to deduce the optimal time between replacements, we designed a mechanism which would create the actual motion of the seat in its normal use. The seat will be raised automatically by the mechanism designed and once it reaches it maximum open position, another mechanism will push the seat past a specific angle so that the seat will close under its own weight. The entire process will be counted as one cycle. Number of cycles, time for moving up the seat (*T1*) and time for seat come back to initial position (*T2*) will be counted by using sensors and a control system. Whenever, *T2* become less than a specified time (this is defined by company) that means the hinges are failing and need to be replaced. The number of cycles for multiple test cases will be recorded which will help deduce the lifetime for these hinges.

2.2 Hinge Specification

Because of equipment inside of this seat (sensors, pump, battery, cleaning foam, etc.), the smart toilet seat used in this paper for analysis weighs over 3kg (heavier than the average

traditional toilet seat). Therefore, the hinges that are used in this smart toilet seat are different than regular hinges. The hinges have an adjustable nut. Tightening or loosening this nut allows the speed of the closing cycle to be adjusted to a desired value.

This hinge is shown in Fig. 3-A. This hinge made of three main parts as it is shown in Fig. 3-B: adjustable nut, head, and tail. Head of the hinge will be attached by a piece to toilet base while tail of the hinge will be attached to the seat. Tightening the adjustable nut causes the head and tail of the hinge to be pressed inside one another that increases the friction between edge of tail (the red dotted part in Fig. 3-B) and edge of the head (the red dotted part in Fig. 3-C). This adjustable nut allows control over the seat closing time under its own weight and can be customized to suit user preferences.

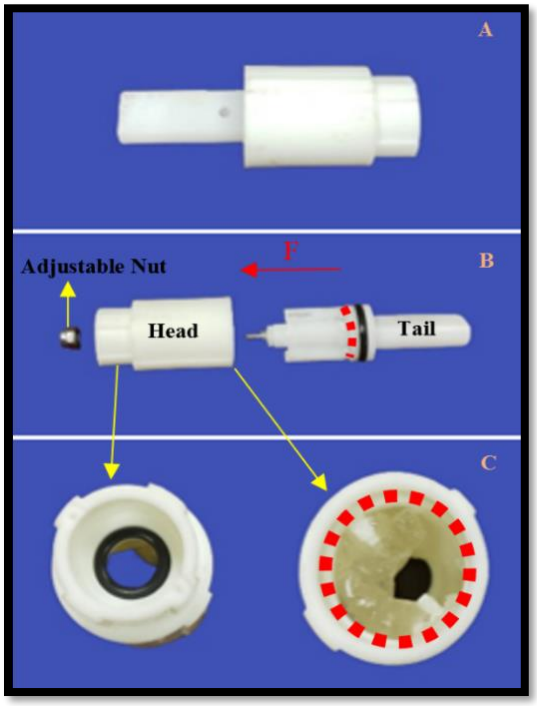

FIGURE 3: A) TOILET HINGE B) DIFFERENT PARTS OF THE TOILET HINGE C) TOP & BOTTOM VIEW OF THE HEAD OF THE HINGE

2.3 Parts of the designed mechanism for the hinge test

As shown in Fig. 4 and mentioned in Table 1, the designed mechanism contains several components.

The mechanism includes (as shown in Fig. 5) a rotational actuator (2), a cable (9), moving frame (14) and several pulleys (3, 4, 8) which together allow raising the seat. A vertical actuator (7), which is used for pushing the seat forward, past a set angle (beyond which the seat will close under its own weight). Several sensors (10, 11, 16) to detect the location of the seat during each part of the entire cycle. The data from these sensors was used to correct the linear or angular displacement for the actuators. All the components are mounted on a structure as shown in Fig. 4.

TABLE 1: LIST OF THE MAIN PARTS FOR THE MECHANISM FOR THE HINGE TEST

#	Parts	Description
1	Fixed Structure	Zinc-Plated Slotted Angle Rods
2	Pulling Up Motor	NEMA 42 CNC Stepper Motor Bipolar 22Nm with 2DM2280 Controller
3	Pulley #1	Bearing Wheel Wire Rope Pulley
4	Shaft Mount	Used to Hold the Steel Rods in Operation
5	Monitor	7 Inches Raspberry Pi Monitor
6	Microcontroller	Arduino Mega 2560
7	Pushing Down Motor	12 Volt Liner Motor with Max Extension of 6 Inches
8	Pulley #2	Bearing Wheel Wire Rope Pulley
9	Cable	Bungee Steel Chord
10	Photo resistors (Light Dependent Resistors (LDR))	Working Voltage: 3 -150VDC
11	Mini Laser Dot Diode Module	Dot Laser Shape, 6 Mm Outer Diameter, 5 Volt, 650nm Wavelength, Less Than 20 Ma Operating Current
12	Toilet Seat	Smart Toilet Seat
13	Toilet Base	Ceramic Toilet
14	Moving Frame	Aluminum Pipes
15	Handle	Aluminum Plate
16	Switch Sensors	Mechanical Limit Switches
17	Power Supply	DC Power Supply for the NEMA-17 Motor

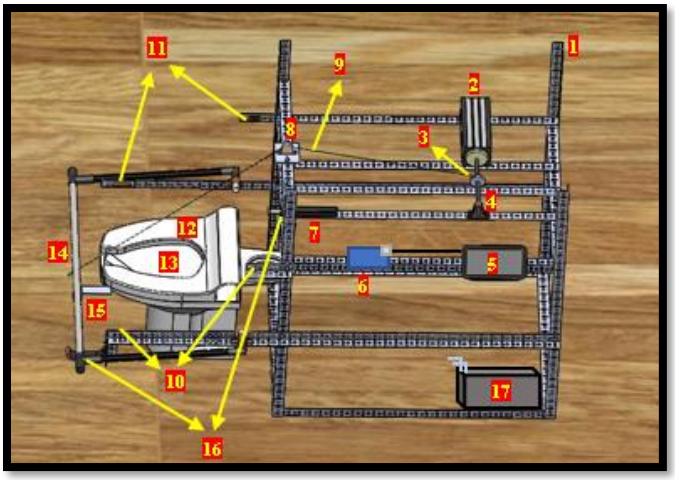

FIGURE 4: MECHANISM MAIN PARTS

An Arduino Mega 2560 microcontroller controls the timing and actuation of the raising-lowering mechanism. A NEMA42 stepper motor is connected to a rotating arm by means of a steel chord. The shaft of the motor is connected to a disc which has the steel chord coiled around it. A clockwise rotation of the disc unwinds the chord, which is required to lower the seat. While a counterclockwise rotation winds the chord, to lift the seat. The chord is passed over a bearing wheel wire rope pulley which is installed midway between the motor and the rotating arm to reduce wear due to friction. The rotating arm lifts the seat to complete the first part of the general segmented process. Two sets of break-beam sensors and laser dot modules are installed. When the light emanating from the laser dots hit the sensors, the circuit is open. When the seat is at the raised position it obstructs the path of the IR beam and closes the circuit. This triggers the linear actuator to push the seat past a specific angle, so that the seat closes under its own weight. The linear actuator is triggered after a time delay, this time delay allows the lifting arm to return to its initial position, so that it does not interfere with the closing of the seat. When the seat cuts off the IR beam, a signal is sent to the microcontroller, this is used for calculating the duration between events. The start and end positions of the two sub-cycles are detected and limited by mechanical limit switches.

2.4 Sensors & Electrical circuit

Fig. 5 shows the specific locations of the sensors to accomplish effective raising and lowering of the seat. To achieve optimal control, to track the position of toilet seat during the cycle and making any corrections required to the lifting mechanism due to the dead time of the electrical motors, six sensors were used at 4 positions.

Two mini laser dot diode modules were used in positions A and B, and two light dependent resistors (LDR) were used as the receivers. This arrangement helps to identify the seat position A – seat open and B - seat closed. Also, two switch sensors, at positions C and D were used to count and correct the number of motor steps. This ensured that the moving frame reached the bottom position and that motor #2 has returned to the initial position and push the switch sensor in position D before a new cycle is started. The inputs from all the sensors, after each trigger event (motion or touching by moving frame) send a signal to the microcontroller which was used to start the next cycle and calculate the time for each cycle. Calculating individual cycle time helped predicting variations in the stiffness of the soft hinge.

The electrical circuit for this system includes the connection between microcontroller, sensors, and motors is shown in Fig. 6.

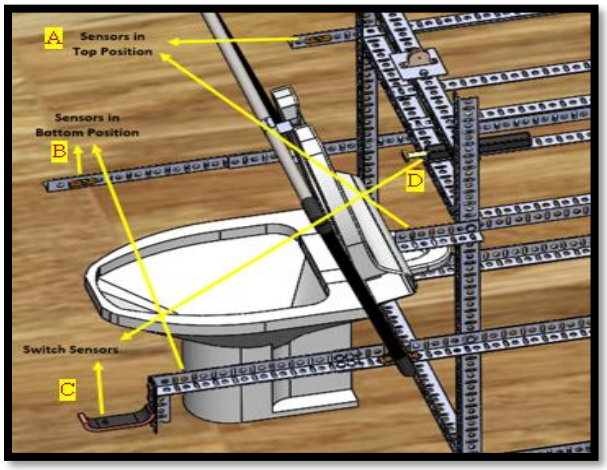

FIGURE 5: LOCATION OF SENSORS IN THE MECHANISM

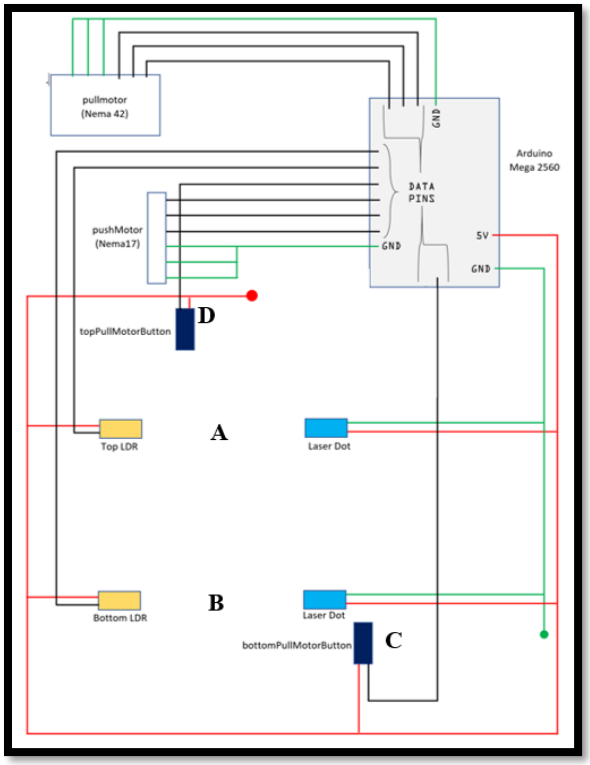

FIGURE 6: ELECTRICAL CIRCUIT FOR THE HINGE TEST MECHANISM

2.5 Mechanism motion study

In this design, we have two motions, one for moving the seat up and then for pushing the seat back down to the original position and be ready for the next cycle.

For the first motion, the seat is raised by an arm which is attached to a moving frame. The moving frame moves from position A to position B. This motion is brough about (Fig. 7) by a cable that passes over two pulleys and is connected Motor #1. Motor #1 is located in the middle of this frame. The time to lift the seat from position A to position B is recorded as (*T1*) for each cycle.

After the seat/arm reaches position B (Fig. 8), the seat would be in a static position, it cannot return to position A on its own. The second half of the overall cycle in our design, uses a linear actuator. This linear actuator labeled Motor #2, pushes the seat past a specified vertical position. Once the seat passes this critical angle the seat returns to position A under its own weight. There is delay written in the software to allow the lifting arm to return to position A before the linear actuator is triggered. To provide redundancy the location of the lifting arm is monitored using a break-beam sensor at A. Once the lifting arm returns to position A it triggers the position sensor at A, letting the microcontroller know when to trigger the linear actuator. The time taken for the seat to travel to position A from position B is recorded as (*T2*) for each cycle.

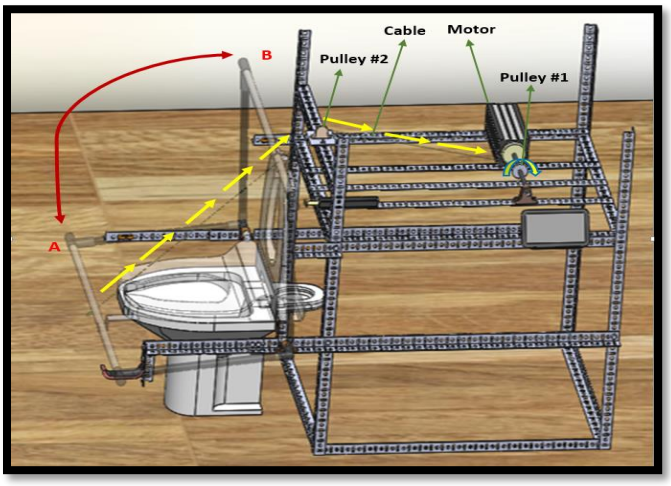

FIGURE 7: MOTION #1 TO CARRY THE SEAT UP

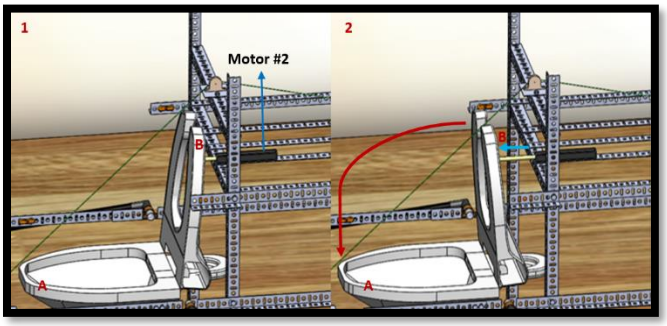

FIGURE 8: MOTION #2 TO PUSH THE SEAT DOWN

3. HINGE TEST RESULTS AND DISCUSSION

Two identical sets of hinges for this smart seat were tested in this round of experiments. A summary of the experimental data is shown in the table below.

TABLE 2: THREE EXPERIMENT SUMMARIES

Experiment		Hinge Set 1	Hinge Set 2
Cycles		17626	14549
Duration		101h 18m 67s	61h 43m 43s
T1	*Max*	3678	4138
	Min	3476	3475
	Mode	3678	3527
	Mean	3655	3683
T2	*Max*	7328	4977
	Min	2157	2217
	Mode	3076	2470
	Mean	3246	3199

Data logging for the experiment on Hinge Set-1 continued with no interruptions in the experimental process until a failure or anomalous signal was noticed. One of the main modes of failure we observed was the hinges became stiff over time and the experiments were stopped. About 21,724 Cycles were registered at the logging terminal.

For Hinge Set-2, there was one interruption during the entire testing period. The data set therefore has a break point in the plot shown in Fig. 9 by a red triangle. The first part of the experiment produced 10,290 Cycles, the second leg of the experiment resulted in 4,264 Cycles and in total, 14,554 Cycles were registered. The interruption was caused due to the need to increase the stroke length of the linear actuator. This was again attributed to the failure mode the hinges exhibited, i.e., stiffening of the hinge.

Another outcome from these experiments, is related to the required time for the seats to fall smooth and slow under their own weight (*T2*). A smooth motion down is important in these seats, as these prototypes have soft-close hinges. Also, since the prototypes house sensors and other electronic components it is essential to reduce the impact due to repeated closing. Preprocessing of the experimental data shows that a few hundred multiple counts were made with Hinge Set-1. This was due to an error in the data logging algorithm. Preprocessing in Microsoft Excel reveals that the Hinge Set-1 produced 17,626 data points and Hinge Set-2 produced 14,549 data points. There were some noises in the raw data from Experiment Hinge Set-1 and Set-2. In Fig.9, to reduce the noise in the raw data, a filter was designed in MATLAB®. The data was plotted again and compared to one another. In this figure, the two sets of data from experiment Hinge Set-2 are sewn together as previously mentioned and highlighted by the red triangle. In Fig.9, the data points for T2 are represented with dots on plot and to have a better observation of their trends. The data sets are fitted with a cubic spline. There

is some similarity between the 2 data sets, specifically between the 1,000th and 8,000th cycles of the experiments. The duration of time T2 continues to reduce for both data sets after this region. However, Hinge Set-1 sees a region of steady values for about 4,000 cycles from the 8,000th cycle until the 12,000th.

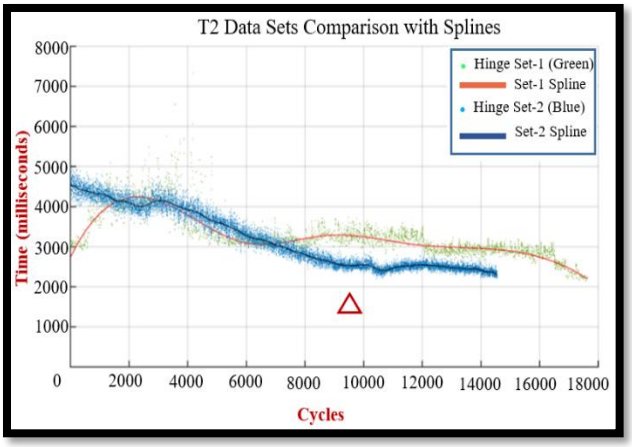

FIGURE 9: T2 DATA SETS COMPARISON WITH SPLINES

In Fig. 10, the splines tracing the data were used to isolate 3 regions of comparability. These have been highlighted for discussion. The first region is from the start of the experiments until about 1,800th cycle. The second region of interest is about the 2,000th to 7,000th cycle and then from the 8,000th cycle to the end of both data sets. The ideal time, for the smart seat going down (T2), would be in the range of 2.5 to 4 seconds and that is related to the weight of the seat and tightness of the hinges. Because the weight of the smart seat is constant, so settings of the hinges is only factor that has effect on T2. The hinges designed for the prototypes can be adjusted to alter the stiffness of the hinge, thereby altering the closing times. In these experiments, based on initial adjustment for the hinge set-1, the seat went down in 3 sec while this time was 4.5 sec for the set-2. However, at the end of stage 1 (transition), the hinge for the set-1 were observed to be stiffer and hinge for set-2 looser, and both started to follow a similar pattern beyond stage 2 (at this point both seats going down in 4 sec). During the stage 2, both hinges became looser based on number of cycles and seats started to move down faster at the end of this stage (3 sec). During stage 3, both hinges kept almost a constant value for time T2 until end of this stage. At the end of this stage, this time drop to less than 2.5 sec which is minimum acceptable range for these hinges, so experiments were stopped.

Both sets of experiments were designed to lift the seat at constant speed. The stiffness of the hinge for the experiment has an effect on the average time it takes to open the seat which would be negligible.

$$mean_{T1} \approx mode_{T1} \approx max_{T1} \approx 3.6\ seconds$$

Fig. 11 shows different steps of actual tests in the lab.

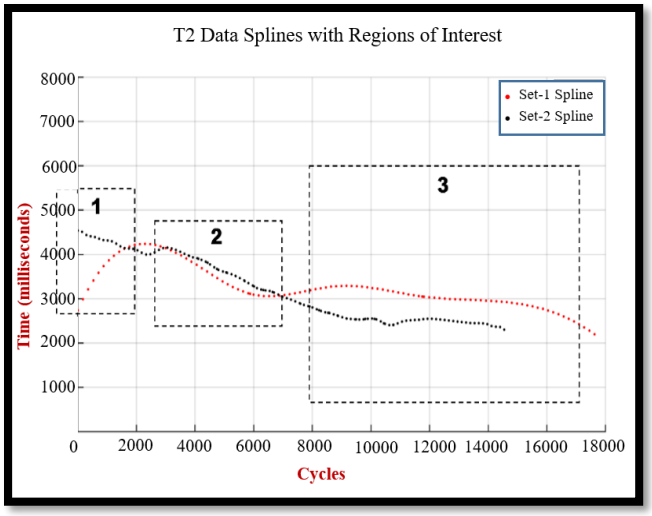

FIGURE 10: T2 DATA SPLINES WITH REGIONS OF INTEREST

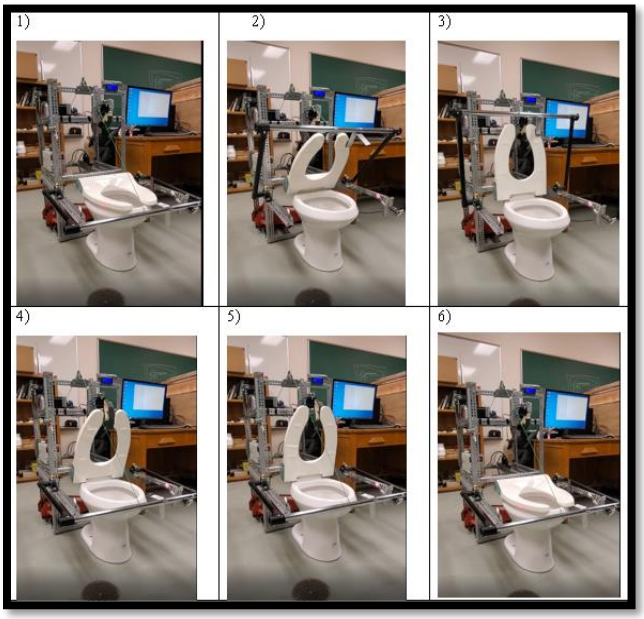

FIGURE 11: PHASES OF THE TEST APPARATUS

4. BATTERY SPECIFICATIONS & DESIGN OF TEST-BED

4.1 Battery & Pump Specification

In this smart toilet seat, a disinfectant foam will be pumped from the top of the seat which the user can use to clean the seat with the provided toilet paper. A motion sensor is located on the side of the seat. The user waves their hand in front of this port, which pumps the disinfectant foam through the opening on the seat. The pump and sensor inside of this toilet seat are powered by 8.57 Volts rechargeable battery. The industry partner

provided us with 3 identical battery packs with same specifications which were to be used for the final product.

4.2 Sensors & Electrical circuit

The lifespan of the battery was approximated by continuously running the pump over an observed period, until the voltage at the battery was so low that it could not trigger the pump mechanism in an adequate fashion (i.e., fails to pump the cleaning solution).

In this experiment, the pump, bottle and battery were detached from the toilet seat and installed in an accelerated test setup. Table 3 and Fig. 12 show the components used in the setup.

Inductive proximity sensors can detect metal objects without touching them and this unique feature can be harnessed and used to detect metallic objects moving perpendicularly in their active detection range. However, because the pump, the pump triggering mechanism and cartridge used in the smart toilet seat are made of plastic, that was not possible. We solved this problem by placing a small metallic object at the tip of the pump mechanism. Therefore, number of retractable motions of the pump tip can be counted by using a microcontroller.

TABLE 3: LIST OF THE MAIN PARTS FOR THE MECHANISM FOR THE BATTERY TEST

#	Parts	Description
1	Inductive Proximity Sensor	Detecting distance: 0-8 mm Voltage: 6-36V Current:30mA Type: NPN (Normally Closed)
2	Microcontroller	Arduino Mega 2560
3	Variable Resistor	Rating: 8k Ohms
4	Resistors	Rating: 100k Ohms, 330 Ohms
5	LCD Display	16x2 Character Liquid Crystal Display
6	Bread Board and Wires	
7	Wooden Setup Frame	Custom Made
8	Sensor Holder	Custom Made

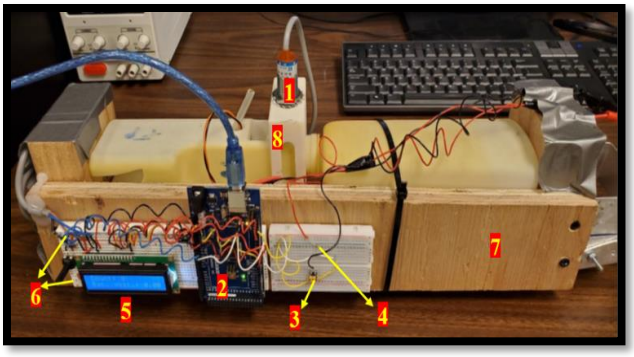

FIGURE 12: BATTERY & PUMP TEST MECHANISM SETUP

In the experimental setup, the aim was to keep count of the number of times the pump displaced from rest to the maximum plunged position, over an observed period of time. It is important to note, that in this setup, the sensor detects and counts the pump twice per cycle which had to be considered in the programming. Arduino Mega 2560 was used in this project for coding the cycles. The circuit wiring diagram is shown in Fig. 13.

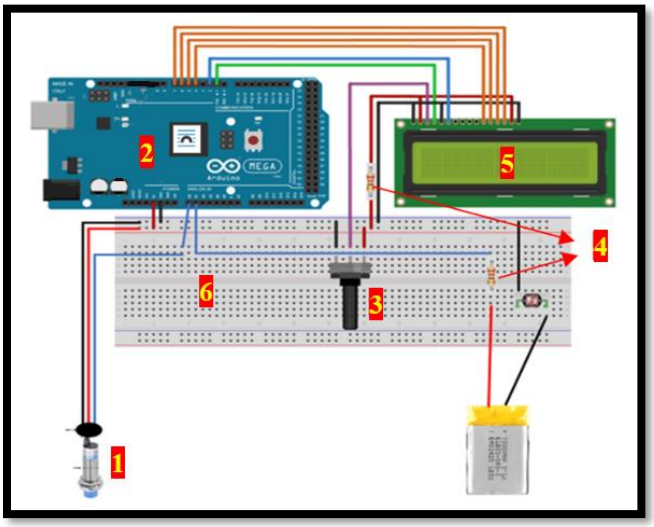

FIGURE 13: ELECTRICAL WIRING DIAGRAM FOR PUMP AND BATTERY TEST

By means of the LCD screen connected as shown in the circuit in Fig. 13, the battery data and pump count were observed throughout the experiment. The variables which were to be collated and recorded are shown in Fig. 14, the values were saved in a tab separated entries format. For each data point, 3 variables were recorded.

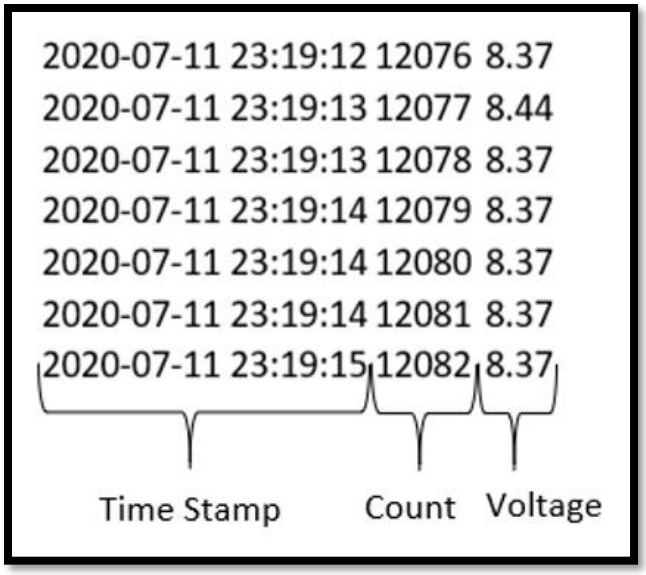

FIGURE 14: DATA LOGGING SAMPLE FORMAT

5. BATTERY TEST RESULTS AND DISCUSSION

The experiments were run for 3 batteries. All batteries had at on an average 200,000 data points. Table 4 shows the summary of the data logged.

TABLE 4: SAMPLE BATTERIES CYCLE DATA

Battery	Data Points	Duration of Accelerated test
A	209741	27 hours, 28 minutes, 8 seconds
B	218251	28 hours, 41 minutes,10 seconds
C	206638	27 hours,1 minute,45 seconds

On pre-processing the data reveals that the minimum useful voltage for the batteries is about 5.87 volts. The median voltage is consistently at 7.84 volts and the battery's longest working voltage is roughly 8.17 volts (Table 5).

TABLE 5: STATISTICS FOR SAMPLE BATTERY RUNS

Voltage (V)	A	B	C
Min	5.87	5.87	4.15
Median	7.84	7.84	7.84
Mode	8.17	8.24	8.17
Max	8.57	8.57	8.57

Fig. 15, plots the battery voltage vs the number of data points. Note the x-axis in the number of pumps cycles (×105) and the y-axis is the battery charge in Volts. The batteries perform exceptionally well and exceeded the industry partner's expectations. The batteries did not show any significant deterioration until the average voltage got to about 7 volts. After this threshold we noticed significant variation in the pump cycle and the time duration to pump. But to reach to 7 V from the maximum average charge of 8.5 V, the batteries were able to run the pump mechanism for about 200,000 cycles. In addition to running the batteries and pump test, we also repeatedly ran multiple charge-discharge cycles to reveal any variations in the maximum charge the batteries could hold. These tests did not result in any deterioration of the batteries nor the maximum charge that they could hold.

At an average, we recorded at least 200,000 useful cycles for these batteries, and the useful lifespan of the battery, before replacement was estimated to be several weeks or months. If we were to make the following conservative assumption: An airport bathroom stall is used on an average for 10 min by a person. In a 24-hour period the number of times that particular stall is used will be (10 min x (24x60) min/day) = 144 times/day and assuming a person would use the cleaning solution (i.e., trigger the pump) at least twice (i.e., 144*2 = 288 times/day). Therefore, they would last 694.44 days (approximately 1 year, 10 months and 25 days) before they need to be replaced. The cartridge on the other hand would run out, on an average in a couple of months. Plus, the pump and all the internal components of the provided cartridges did not fail during any of the tests conducted.

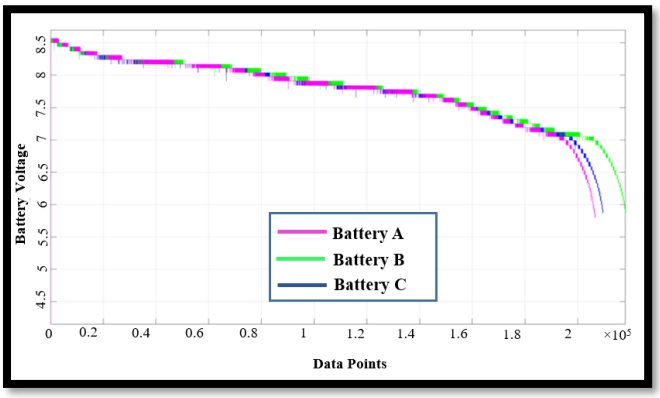

FIGURE 15: BATTERY TEST DATA FOR THREE SAMPLE BATTERIES

6. CONCLUSION

In this work, lifetime for custom-designed hinges and batteries of a smart toilet seat were tested and analyzed. We used Accelerate Life Testing (ALT) method for each of these tests. A special mechanism was designed to test the useful lifespan of the hinge and to study the failure modes. For the hinge test, time required for opening and closing the seat plus the total number of cycles before the hinge fails was counted and reported. For the battery test, the total number of pumping cycles were counted. This test helped identify the lowest voltage that the battery could operate at. These tests were repeated with two different samples

for hinge and 3 different production certified battery units and results were compared. Final results showed, on an average the hinges after 14,000 cycles and batteries after 200,000 cycles have to be replaced which could be considered as a good lifetime for these parts of the smart toilet seats even if the seats will be utilized in the public places like airports.

REFERENCES

[1] B. Orlando, F. De Carlo, N. Fanciullacci and M. Tucci, 2013. Accelerated life tests for new product qualification: A case study in the household appliance. Proc. of the 11th IFAC Workshop on Intelligent Manufacturing Systems, Sao Paulo, Brazil.

[2] W. Nelson, 1974. A survey of methods for planning and analyzing accelerated tests. IEEE transaction on Electrical insulation, EI-9 (1), 12-18.

[3] C. Jeffrey, U. Garganese and R. Swarz, 1997. An Approach to Designing Accelerated Life-Testing Experiments. IEEE 1997 proceedings annual reliability and maintainability symposium

[4] A. F. Attia, H. M. Aly, and S. O. Bleed, 2011. Estimating and Planning Accelerated Life Test Using Constant Stress for Generalized Logistic Distribution under Type-I Censoring. International Scholarly Research Network ISRN Applied Mathematics Volume 2011, Article ID 203618, 15 pages, doi:10.5402/2011/203618

[5] R. Moeller, T. Deemyad, and A. Sebastian, 2020, October. Autonomous Navigation of an Agricultural Robot Using RTK GPS and Pixhawk. In 2020 Intermountain Engineering, Technology and Computing (IETC) (pp. 1-6). IEEE.

[6] Á. Wolf, M. Paul, P. Galambos, and K., Széll, 2020, September. Detecting Gripping Failure in a Liquid Handling Robot with a Break Beam Sensor. In 2020 IEEE 18th International Symposium on Intelligent Systems and Informatics (SISY) (pp. 101-106). IEEE.

[7] T. Deemyad, R. Moeller, and A. Sebastian. "Chassis Design and Analysis of an Autonomous Ground Vehicle (AGV) using Genetic Algorithm". In Intermountain Engineering, Technology, and Computing Conference (i-ETC). IEEE, 2020.

[8] T. Deemyad, N. Hassanzadeh, and A. Perez-Gracia. Coupling mechanisms for multi-fingered robotic hands with skew axes. In Mechanism Design for Robotics (MEDER). Springer, 2018.

[9] T. Deemyad, O. Heidari, and A. Perez-Gracia. Singularity Design for RRSS Mechanisms. In USCToMM Symposium on Mechanical Systems and Robotics (MSR) Conferences. Springer, 2020.

[10] Y.S. Krieger, C.M. Kuball, D. Rumschoettel, C. Dietz, J.H. Pfeiffer, D.B. Roppenecker, and T.C. Lueth, 2017, September. Fatigue strength of laser sintered flexure hinge structures for soft robotic applications. In 2017 IEEE/RSJ International Conference on Intelligent Robots and Systems (IROS) (pp. 1230-1235). IEEE.

[11] W. Wang, N.G. Kim, H. Rodrigue, and S.H. Ahn, 2017. Modular assembly of soft deployable structures and robots. Materials Horizons, 4(3), pp.367-376.

[12] M.S. Hosen, J. Jaguemont, J. Van Mierlo, and M. Berecibar, 2021. Battery lifetime prediction and performance assessment of different modeling approaches. Iscience, 24(2), p.102060.

[13] Z. Fei, F. Yang, K.L. Tsui, L. Li, and Z. Zhang, 2021. Early prediction of battery lifetime via a machine learning based framework. Energy, 225, p.120205.

[14] Y.C. Yin, F.P. Coolen, and T. Coolen-Maturi, 2017. An imprecise statistical method for accelerated life testing using the power-Weibull model. Reliability Engineering & System Safety, 167, pp.158-167.

[15] W. Nelson, 1980. Accelerated life testing-step-stress models and data analyses. IEEE transactions on reliability, 29(2), pp.103-108.

[16] S. Habibian, M. Dadvar, B. Peykari, A. Hosseini, M.H. Salehzadeh, A.H. Hosseini, and F. Najafi, 2021. Design and implementation of a maxi-sized mobile robot (Karo) for rescue missions. ROBOMECH Journal, 8(1), pp.1-33.